

Research Article



Check for updates

OPEN

Development of a Fluorescence Immunoassay Based on Curcumin Carbon Dots-labeled IgY Antibodies for SARS-CoV-2 Detection

Nisa Amanda Rachmadani¹, Meilisa Keizia Soetomo², Audrey Angelina Putri Taharuddin², Arum Sinda Santika³, Oktaviardi Bityasmawan Abdillah^{3,4}, Fitri Aulia Permatasari^{3,4,5}, Ferry Iskandar^{3,4,5}, Heni Rachmawati^{5,6}, Azzania Fibriani^{2,5*}

¹Department of Nanotechnology, Graduate School, Institut Teknologi Bandung, Bandung 40132, Indonesia

²School of Life Sciences and Technology, Institut Teknologi Bandung, Bandung 40132, Indonesia

³Department of Physics, Faculty Mathematics and Natural Sciences, Institut Teknologi Bandung, Bandung 40132, Indonesia

⁴Collaboration Research Center for Advanced Energy Materials, National Research Innovation Agency - Institut Teknologi Bandung, Bandung 40132, Indonesia

⁵Research Center for Nanoscience and Nanotechnology, Institut Teknologi Bandung, Bandung 40132, Indonesia

⁶School of Pharmacy, Institut Teknologi Bandung, Bandung 40132, Indonesia

ARTICLE INFO

Article history:

Received February 11, 2025

Received in revised form April 27, 2025

Accepted June 9, 2025

Available Online October 6, 2025

KEYWORDS:

carbon dots,
fluorescence,
lateral flow assay,
nano-bioconjugation,
SARS-CoV-2

ABSTRACT

Carbon dots (CDs) are widely utilized in biomedical applications as fluorescent labels for imaging and diagnostics due to their excellent biocompatibility and superior optical properties. These advantages often make CDs a substitute for organic fluorescent dyes, which suffer from low emission intensity and poor photostability when interacting with biomolecules. Moreover, carbon-based materials are eco-friendly and can be synthesized from natural sources, such as curcumin, a chromophore compound abundantly available in Indonesia. Therefore, this study conducted a preliminary investigation on curcumin CDs-labeled IgY antibodies (IgY-cur CDs) for fluorescence immunoassay of SARS-CoV-2 in rapid test applications. The synthesis of the fluorescent label involved a carbodiimide coupling reaction using EDC/NHS agents to conjugate IgY antibodies with curcumin CDs. The IgY-cur CDs conjugate was confirmed to detect antigens through FRET immunosensor mechanisms, showing a significant increase in fluorescence intensity with increasing antigen concentrations ($p < 0.05$), with a minimum sample concentration of 10 ng. Furthermore, the IgY-CDs cur conjugate was applied as a reporter in a fluorescence-based LFIA using a sandwich assay format. The test strip successfully detected synthetic multiepitope SARS-CoV-2 antigens with an estimated detection limit of 54.28 μ g and nasopharyngeal samples from confirmed COVID-19 patients within 35 minutes of operation. The test strip was evaluated to be stable under cold storage at 4°C for up to 3 weeks. In conclusion, curcumin CDs-labeled IgY antibodies demonstrate promising potential for further development as fluorescent labels in rapid diagnostic applications targeting SARS-CoV-2.



Copyright (c) 2026 @author(s).

1. Introduction

Pathogenic viral infections have become a significant global health threat in recent years,

particularly during the coronavirus disease 2019 (COVID-19) pandemic. After four years of the pandemic, the World Health Organization (WHO) officially announced that the COVID-19 emergency had ended in May 2023. However, WHO also advised every country to transition to long-term management

* Corresponding Author

E-mail Address: afibriani@itb.ac.id

of the COVID-19 pandemic, considering uncertainties posed by the potential evolution of Severe Acute Respiratory Syndrome-Coronavirus-2 (SARS-CoV-2). In line with these guidelines, the WHO suggested that each country must have a preparedness plan to prevent panic and negligence, as pandemic outbreaks cannot be predicted. Thus, the development of rapid and selective pathogen detection technology is a significant effort to prepare for pandemics, as well as future epidemics and endemics.

Recently, a growing interest has emerged in developing fluorescence immunoassay for various purposes, such as nucleic acid (Borghesi *et al.* 2018), protein (Deb *et al.* 2023), and toxins produced in bioproducts (Tang *et al.* 2020) also along with environmental pollutants (Pan & Xinlin 2022). In addition to these applications, fluorescence-based immunosensors are promising for use as rapid detection methods. Examples include fluorescence resonance energy transfer (FRET) and lateral flow assay (LFA). A FRET immunosensor is a type of biosensor that utilizes the principle of protein binding, where the target biomolecules interact explicitly, and the FRET signal is used to detect these binding events. Unlike conventional ELISA, it can detect target analytes quickly due to the fast and highly sensitive monitoring of nano-bio interactions at very low concentrations, such as nanomolar and picomolar levels (Verma *et al.* 2023). Making it suitable for point-of-care diagnostics and rapid screening procedures in various biosensing applications (Pan & Xinlin 2022).

The development of fluorescence-based LFA is an intriguing topic for exploration. LFA is an immunochromatographic assay and uses gold nanoparticles as standard labels. However, gold colloid-based LFA often faces challenges, such as a limited detection range, which can affect sensitivity and accuracy. As a result, researchers have increasingly substituted colorimetric markers with non-colorimetric markers, such as fluorescence (Wang *et al.* 2019; Tang *et al.* 2021; Ju *et al.* 2022). The selection of labels for use in LFIA involves careful consideration of specific criteria. Nanoparticle labels must meet several conditions, including stability, a wide dynamic detection range, minimal impact on nonspecific binding, and availability as commercially viable materials at a low cost (Koczula & Gallotta 2016).

Carbon dots (CDs) are ideal for fluorescent labels due to their high quantum yield and multi-

color properties (Xu *et al.* 2021). In biomedical research, CDs are favored due to their excellent water solubility, biocompatibility, and ease of functionalization (Bhushan *et al.* 2016; Kuznetsova 2023). Furthermore, carbon-based materials are more environmentally friendly than quantum dots, typically made from heavy metals. CDs can be synthesized from natural materials and byproducts (Huang *et al.* 2019; Raveendran & Kizhakayil 2021). From an economic perspective, CDs offer simple production methods and are inexpensive. Based on these advantages, curcumin-based CDs are promising candidates for fluorescence immunosensors. Notably, there have been no studies on curcumin CDs targeting SARS-CoV-2 antigens in LFA.

Therefore, in this study, we designed the development of specific SARS-CoV-2 spike and NS3 polypeptide-based polyclonal IgY antibodies labeled with curcumin CDs as reporters for rapid detection. The selection of polyclonal IgY antibodies based on multiepitope SARS-CoV-2 peptides, produced according to protocols outlined in previous research (Fibriani *et al.* 2022, 2025), is considered an alternative to IgG as a component of immunoassays. The conjugation of IgY antibodies with curcumin-derived CDs as labels was performed through carbodiimide coupling reactions using EDC/NHS agents. Subsequently, the IgY-CDs conjugates were evaluated in a rapid test construct to assess their stability and sensitivity against synthetic antigen samples as well as COVID-19 patient samples. The concept designed in this study aims to discover the performance of curcumin-derived CDs as a candidate for fluorescence labels in LFA as a research scheme (Figure 1).

2. Materials and Methods

All experimental stages in this study were conducted as wet-lab experiments from November 2023 to November 2024 at the Genetics and Molecular Laboratory and BSL-2 facilities at Institut Teknologi Bandung.

2.1. Materials and Reagents

Citric acid, urea, and 2-(N-morpholino)ethanesulfonic acid (MES) were purchased from Sigma-Aldrich, USA. Curcumin was procured from Combiphar, Indonesia. 1-Ethyl-3-(3-dimethyl aminopropyl) carbodiimide hydrochloride (EDC) and N-hydroxysuccinimide

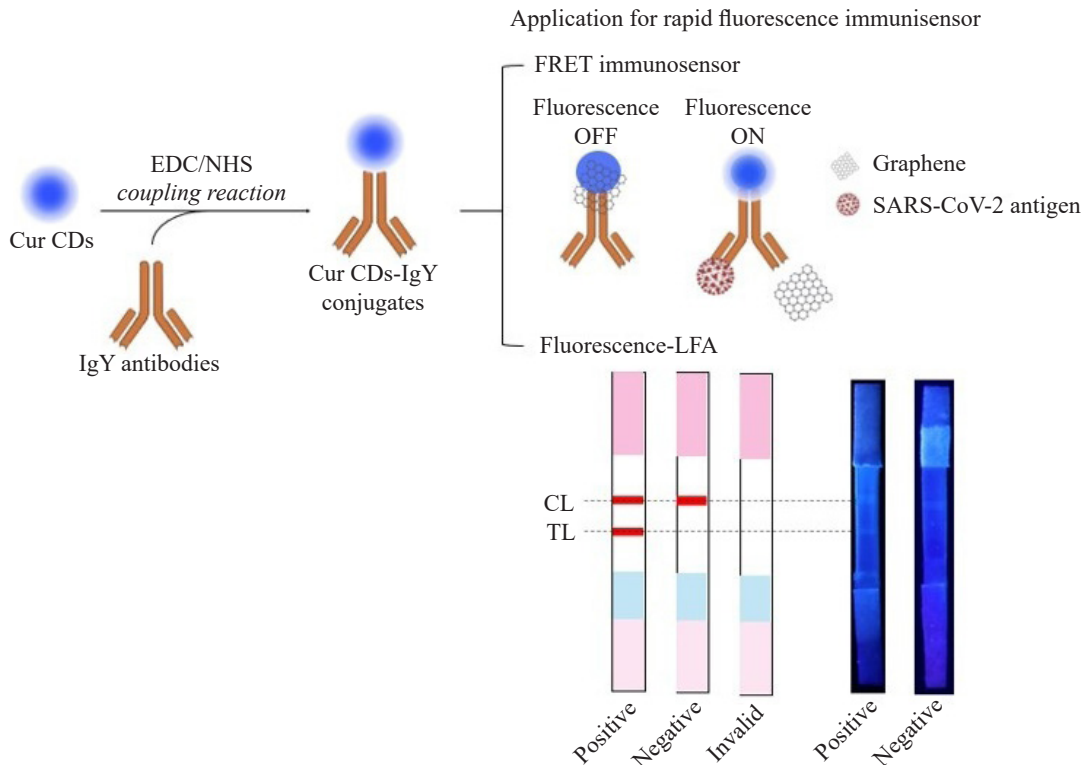


Figure 1. Research scheme overview in this study designed two approach for rapid fluorescence immunoassay

(NHS) were purchased from Thermo Scientific, USA. Phosphate-buffered saline (PBS) and ammonium sulfate ($(\text{NH}_4)_2\text{SO}_4$) were purchased from Merck, India. Another reagent used in this research is 50% hydrogen peroxide (H_2O_2) from Bratachem, concentrated sulfuric acid (H_2SO_4) from Smartlab, Indonesia, deionized water, and 70% ethanol. The consumption materials are graphite sheet procured from Hi-tech Carbon, Ltd., NanoComposix LFIA starter kit (Lot No. JLC0142), Hi-Flow Plus HF180 membrane cards, goat anti-chicken IgY, multiepitope spike and NS3 SARS-CoV-2 antigen and IgY polyclonal antibody specific spike and NS3.

2.2. Ethics Approval

The nasopharyngeal swab sample was collected from the Health Laboratory of West Java Province, Indonesia, and was used solely for scientific research, which the Research Ethics Committee of Padjajaran University approved.

2.3. Curcumin CDs Synthesis

Curcumin CDs (Cur CDs) were synthesized using the previously described method via the solvothermal route, as reported in the previous study. Citric acid, urea, and curcumin are used as precursors. The precursor was

reacted in a Teflon autoclave at 160°C with a pressure of 0.8-1.0 MPa for 300 minutes. After forming the solution, it was filtered using a regenerated cellulose filter membrane with a 0.2 μm pore size and purified through centrifugation at 4000 rpm for 30 minutes. The cur CDs were obtained after dry freezing (Fibriani *et al.* 2023).

2.4. Synthesis of Graphene Nanosheets

Graphene nanosheets in this study were synthesized from graphite sheets using an electrochemical exfoliation process (Abdillah *et al.* 2020). Graphite sheets were pre-treated in a 95:5 vol% $\text{H}_2\text{SO}_4:\text{H}_2\text{O}_2$ solution for 3 minutes to produce the expanded graphite sheet. In the electro-exfoliation process, a pre-treated graphite sheet and a Pt wire were used as the working electrode and counter electrode, respectively, in 100 mL of an aqueous $(\text{NH}_4)_2\text{SO}_4$ (0.1 M) electrolyte. The electrodes were subjected to a constant potential bias of 10 V until no further current could be detected. After that, the exfoliated product was washed with deionized water using vacuum filtration until a pH of 7.0 was achieved, and then it was dried at 40°C for 6 hours. The product was then dispersed in deionized water using an ultrasonic homogenizer (pulsed at 480 W) for an hour to break

down exfoliated graphite into graphene nanosheets. The dispersion was centrifuged at 1000 rpm for 20 minutes to separate large particles from the dispersion. The supernatant resulting from centrifugation was dried at 80°C overnight to obtain the final product of the graphene nanosheets.

2.5. Nano-bioconjugation of Curcumin CDs and IgY Antibodies

Bioconjugation of Cur CDs and polyclonal IgY antibodies specific to the SARS-CoV-2 spike and NS3 proteins is performed using a carbodiimide coupling reaction. EDC (10 mg/mL) and NHS (15 mg/mL) reagent coupling was prepared in 0.1 M MES buffer, pH 5.5. 600 µL of Cur CDs solution (1.5 mg/mL) was incubated with 200 µL of EDC and 150 µL of NHS for 20 minutes, respectively. After that, an antibody (300 µg) was added to the previous reaction. The mixture was shaken at a speed of 800 rpm for 2 hours at 25°C in the dark and then preserved overnight at 4°C for complete covalent binding of antibodies to the Cur CDs surface. Then, the sample was centrifuged at 3500 rcf for 5 minutes and filtered using a 10 kDa filtration membrane to eliminate unreacted ingredients. Cur CDs-IgY conjugates concentrate was diluted to the initial volume with PBS and can be stored at 4°C.

2.6. Characterization of Nano-bioconjugation Result

The conjugation results of Cur CDs and polyclonal IgY antibodies were characterized by low-resolution transmission electron microscopy (LR-TEM), Fourier transform infrared spectroscopy (FTIR), and fluorescence spectroscopy. The size distribution of the material was calculated with ImageJ, and the spectrum data were analyzed with OriginLab software.

2.7. FRET Immunosensor

The FRET immunosensor in this study was used as a method to confirm the detection activity of the curcumin IgY-CDs antibody conjugate against the SARS-CoV-2 multiepitope antigen. 100 µL of curcumin carbon dots conjugated polyclonal antibody was incubated with 10 µL of graphene (75 µg) and shaken for 15 minutes at room temperature. After that, 100 µL of synthetic multiepitope spike and NS3 SARS-CoV-2 antigens were added, and the mixture was shaken again for an additional 45 minutes at 37°C with a speed of 300 rpm. Fluorescence values were measured using a GloMax microplate reader with an excitation wavelength of UV 365 nm and an emission range of 415-445 nm.

2.8. Fabrication of Fluorescence-based LFA Strips

First, the test line on a nitrocellulose membrane was prepared by immobilizing IgY specific to the SARS-CoV-2 spike and NS3 (3 mg/mL), while goat anti-IgY antibodies (2 mg/mL) served as the control line, marked with the tip of a double-headed marker. The conjugate pad was incubated with the Cur CDs-IgY conjugate solution, and the sample pad underwent non-woven treatment using PBS containing 1% Triton X as the running buffer for immobilization. Then, the sample pad and conjugate pad were dried at 37°C for 12 hours, while the nitrocellulose membrane was re-immobilized and dried again for 12 hours. The component of the fluorescence LFIA was assembled overlapping on a backing card to ensure that the test solution could migrate through the strip (Figure 2). The entire assembled card was cut into 0.5 cm-wide strips and stored in a sealed bag with desiccant. A positive result was indicated by the appearance of a glowing blue line on both the test and control lines, whereas a negative result showed a glowing blue line only on the control line under UV light.

2.9. Stability and Sensitivity Test

The performance evaluation of the test strip was conducted by assessing its limit of detection, stability, and sensitivity. The strip was tested using analytes containing synthetic SARS-CoV-2 antigens at concentrations of 0 µg, 5 µg, 10 µg, 25 µg, 50 µg, 75 µg, and 100 µg. Stability tests were performed periodically during storage at room temperature (25°C) and cold storage (4°C). Sensitivity testing involved analyzing samples from patients confirmed to have COVID-19. Each test type uses strips from the same production batch to ensure consistency.

3. Results

3.1. Curcumin CDs and IgY Antibodies Conjugates Characterization

The results of the nano-bioconjugation of curcumin carbon dots (Cur CDs) with IgY, achieved through the carbodiimide carboxylamine coupling method, were characterized using various techniques, including morphological analysis, fluorescence studies, and identification of functional groups. Their morphological analysis was performed using LR-TEM (Figure 3a). The red arrow on the LR-TEM image indicated a spherical shape with an average diameter of approximately 2.3 nm, characterized by an island-like amorphous structure.

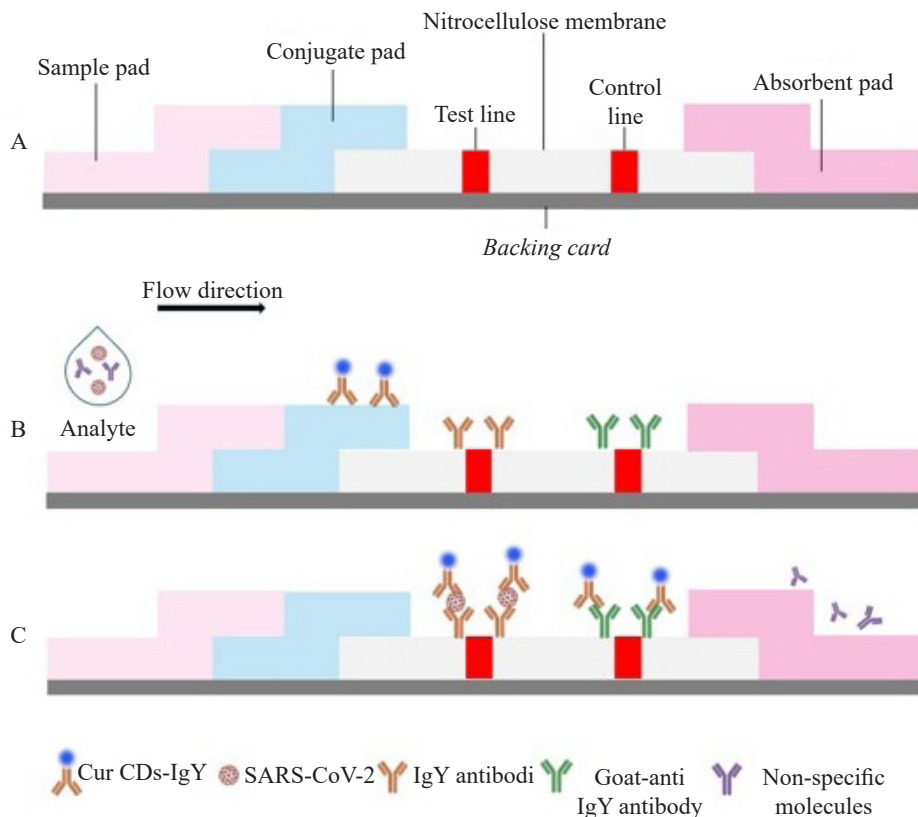


Figure 2. Schematic illustration the configurations of fluorescence-based test strip. (A) Component of LFIA, (B) LFIA construction, and (C) the detection of SARS-CoV-2 antigen

The diameter increased to 15 nm after bioconjugation with IgY (Figure 3b). This size increase is due to the binding between Cur CDs and the IgY complex, as well as the reagents used during the coupling reaction. The conjugation solution appeared yellow-brownish under visible light and exhibited blue fluorescence under UV light. The fluorescence analysis of as-prepared Cur CDs is shown in an excitation range of 200-500 nm. We can clearly state that the optical properties of CDs are an excitation-dependent phenomenon (Figure 4a). Furthermore, in Figure 4b, Cur CDs and Cur CDs-pAb exhibit fluorescence emission at a 365 nm excitation wavelength.

The fluorescence characteristics of curcumin CDs were also evaluated in relation to pH levels to determine the optimal conditions. After the coupling reactions, the pH of the curcumin CDs was 6, which was considered optimal because the highest fluorescence intensity of Cur CDs was observed in the pH range of 5 to 6 (Figure 5). To confirm the functional group change, FTIR analysis was applied (Figure 6). The FTIR peaks analysis of Cur CDs showed at 1320 cm^{-1} , 1437 cm^{-1} , 1559 cm^{-1} , 1648 cm^{-1} , and 3150 cm^{-1} which were attributed to COO^- ,

C-N , $\text{C}=\text{C}$, $\text{C}=\text{O}$, and $\text{O}-\text{H}$, respectively. These functional groups are observed in both CDs and Cur CDs-pAb, while the COOH group was only found in CDs-pAb. The absorption band of $-\text{COOH}$ was observed at 1773 cm^{-1} in the FTIR peaks of Cur CDs-conjugates, indicating covalent coupling.

3.2. FRET Immunosensor

The Cur CDs-IgY conjugate was evaluated for its effectiveness as a probe in the detection of SARS-CoV-2 antigens using the FRET immunosensor method. To investigate the quenching effect of graphene nanosheets as an acceptor of Cur CDs-IgY fluorescence in this system, several concentrations with various incubation times were examined. A $75\text{ }\mu\text{g}$ concentration of graphene nanosheets with a 15-minute incubation time was selected for subsequent experiments. In the FRET immunosensor results (Figure 7), the graphene nanosheet can quench 33% of the fluorescence intensity of Cur CDs conjugate (in the absence of antigen) compared to the control Cur CDs-IgY conjugate. The addition of $30\text{ }\mu\text{g}$ of antigen to the FRET system restored the fluorescence intensity by 52%, which was even higher than the initial fluorescence

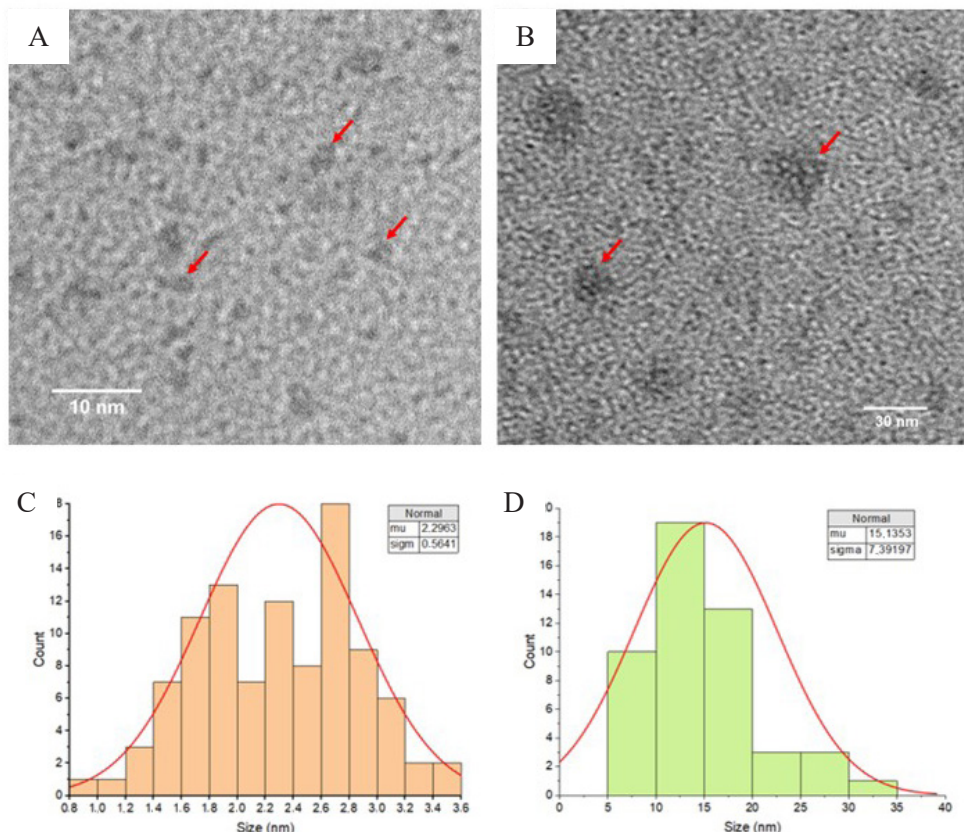


Figure 3. The LR-TEM analysis results show (A) Cur CDs before and (B) after conjugation with IgY antibodies. The red arrows indicate the specific material being referenced. The size distribution (C) of Curcumin CDs is approximately 2.3 nm, whereas (D) the CDs-IgY conjugate is around 15 nm

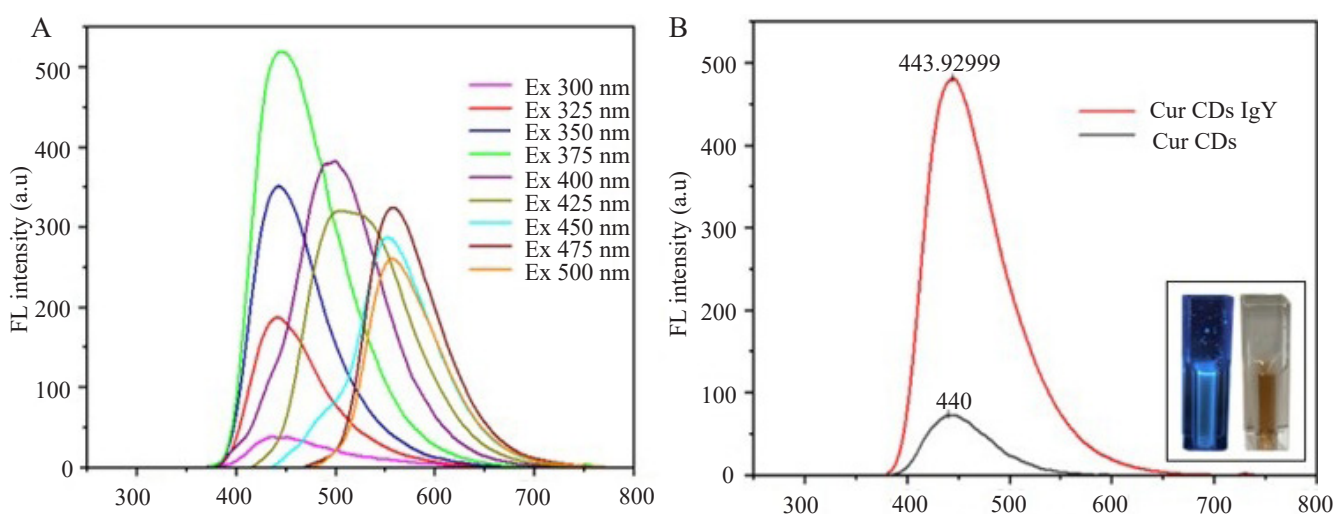


Figure 4. The fluorescence emission spectra of (A) Cur CDs-IgY conjugates over an excitation wavelength of 200-500 nm, and (B) comparison between Cur CDs at 365 nm excitation. The inset shows images of Cur CDs-IgY under visible light and UV

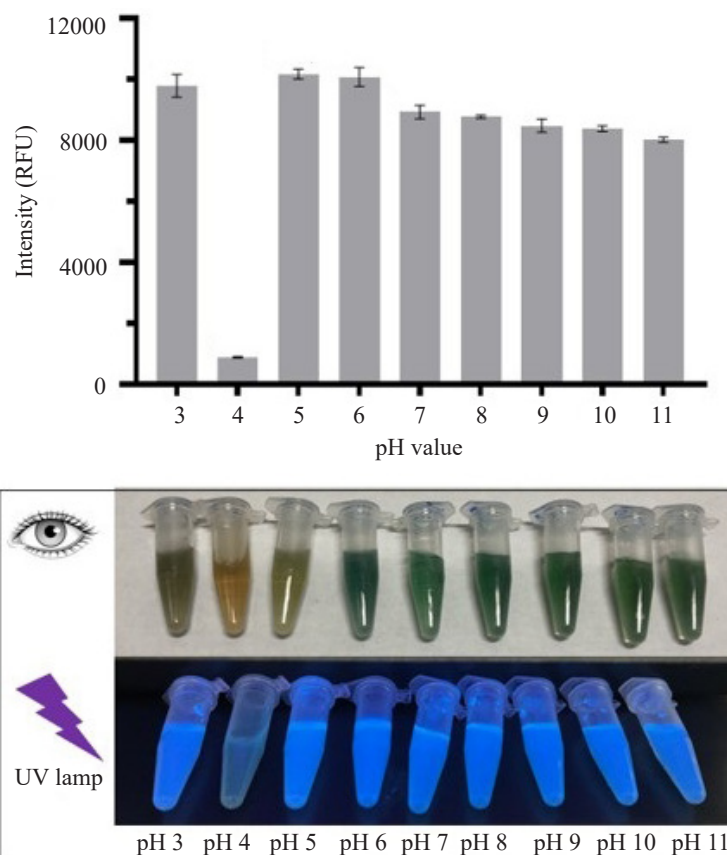


Figure 5. Fluorescence characteristics of Cur CDs based on pH levels. Shown through fluorescence intensity values and visual representation

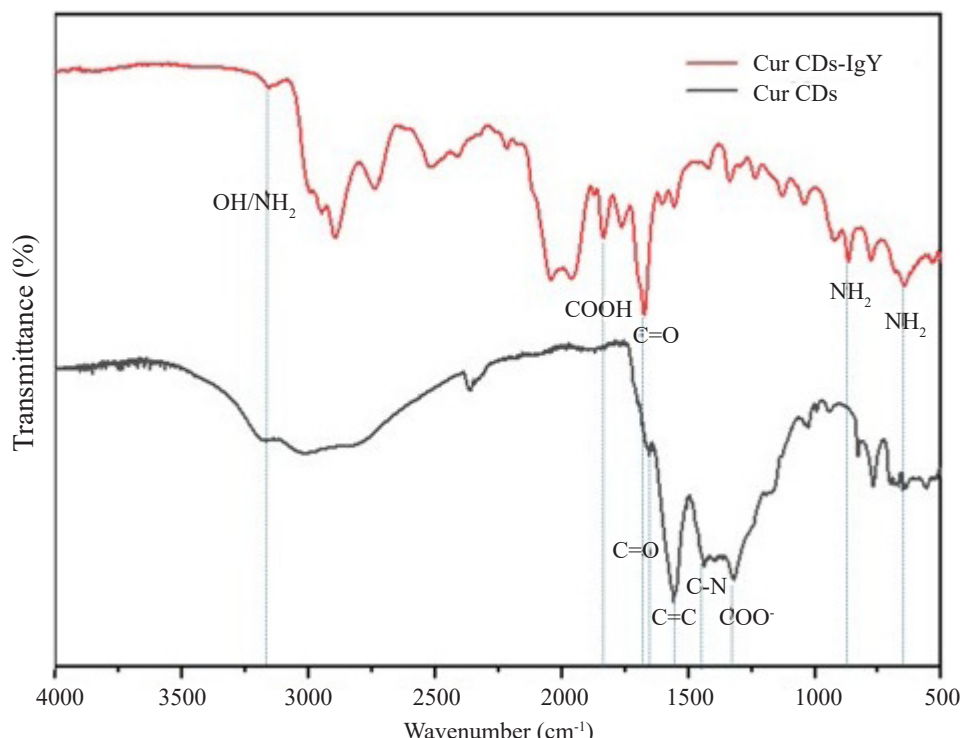


Figure 6. FTIR analysis of Cur CDs before and after conjugation with IgY antibody. Cur CDs-IgY revealed the absorption band of -COOH

intensity of the control Cur CDs-IgY conjugate. Statistical analysis represented by asterisks showed that the fluorescence intensity, based on a One-way ANOVA test, was highly significant with a p -value <0.05 . Thus, the FRET immunosensor approach confirms that the IgY-curcumin CDs conjugate has potential as a fluorescence probe for SARS-CoV-2 detection.

Serial dilution of multiepitope synthetic antigens SARS-CoV-2 was carried out in the range of 1 to 1000 ng to identify the sensitivity performance of IgY-Cur CDs in the

FRET immunosensor system. It is known that eight types of antigen concentration treatments showed an increase in fluorescence intensity as the concentration of the loaded antigen increased. The dose-response curve (Figure 8) was created by plotting the normalized fluorescence intensity (F/F_0), where F_0 represents the intensity of the control mixture, which is sterile PBS without antigen, and F is the fluorescence intensity at each antigen concentration. A dose-response curve is constructed by plotting the fluorescence intensity as a function of the logarithm of the

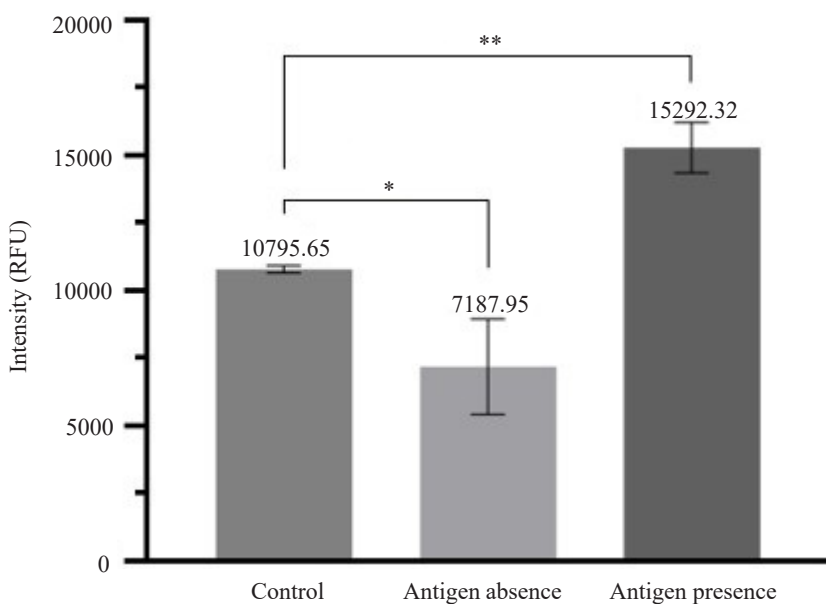


Figure 7. FRET immunosensor validation. The PL intensity in the absence and presence of antigen compared to control but showed a significance value (* $p<0.05$, ** $p<0.001$)

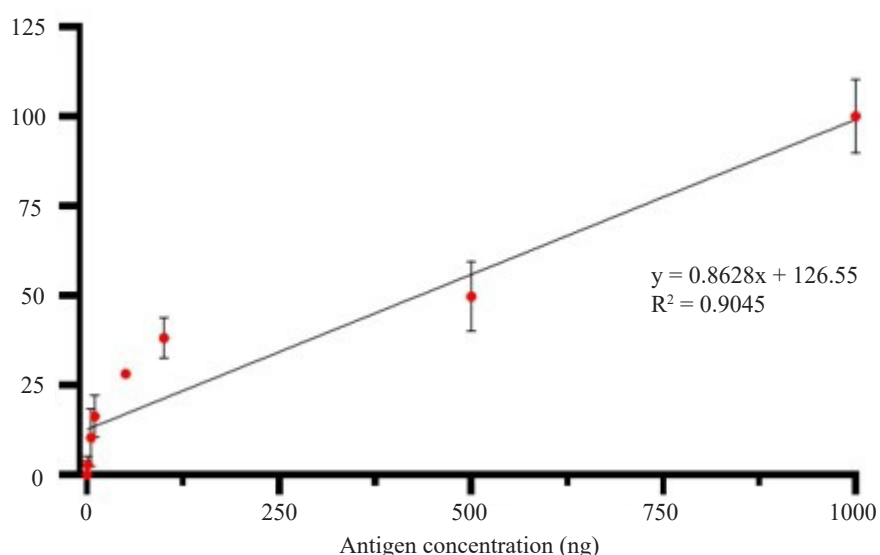


Figure 8. Corresponding plot of fluorescence intensity of Cur CDs-IgY in FRET immunosensor with graphene in the existence of various Log numbers of viral antigen, detection range 1-1000 ng

viral antigen concentration. The simple linear regression equation is expressed as $y = 0.8628x + 126.55$, with a strong correlation ($R^2 = 0.9045$), indicating that the model predicts 90% of the relationship.

3.3. Fluorescence-based LFA

To explore the feasibility of Cur CDs as fluorescence labels on the strip test. The first was to conjugate Cur CDs with IgY antibody. The optimization of the construct was performed with two types of variations: conjugate pad variations and test lines. The assembled strips were then tested for feasibility using PBS as a control sample and synthetic multiepitope antigens (specific to spike and NS3) of SARS-CoV-2 as positive samples. The purpose of this two-variation optimization was to evaluate the flow rate, which would ultimately impact the optimal testing performance.

The first variation, the Cur CDs-IgY conjugates, are grouped into 2 types of preservation. There are Cur CDs-IgY preserved with 5% BSA and without it. The feasibility test using Cur CDs-IgY antibody without BSA preservation on a conjugate pad was selected for further investigation because the presence of BSA affects the flow viscosity (Figure 9). Therefore, the LFIA construction was then modified with a variation of the conjugate pad containing Cur CDs-IgY without BSA preservation. The second variation, construct optimization, was carried out by varying the pH of the IgY antibodies immobilized on the test line on the nitrocellulose membrane.

pH variations of 6.0 and 7.4 were applied to the nitrocellulose membrane, and the test line fluorescence was found not to be significantly different from that observed by the eye. Thus, a variation of the conjugate pad construction containing CDs-labeled IgY antibodies without BSA preservation and pH 7.4 IgY antibodies was selected to be immobilized on the nitrocellulose membrane as a test line for further strip construction.

The sensitivity performance of the fluorescence-based LFA was evaluated against synthetic SARS-CoV-2 antigens. The test employed a sample concentration range of 5 to 100 $\mu\text{g}/\text{mL}$, with measurements taken in triplicate. Images of the nitrocellulose membrane were captured 35 minutes post-sample loading, and fluorescence intensity was analyzed using image J (Figure 10). The fluorescence intensity of the test line increased proportionally with the increasing concentration of SARS-CoV-2 antigen. Lower concentrations showed weaker fluorescence due to inconsistent biomolecule immobilization and background reflection. The test demonstrated a linear relationship between fluorescence intensity and antigen concentration, yielding a strong correlation coefficient ($R^2 = 0.9838$) and a detection limit prediction of 54.28 $\mu\text{g}/\text{mL}$.

The strip's performance was further evaluated for stability under various storage temperatures over four weeks. Assembled test strips were stored in aluminum bags with silica gel at room temperature (25°C) and in cold storage (4°C). All strips were produced in the same batch and tested weekly using synthetic antigens at the

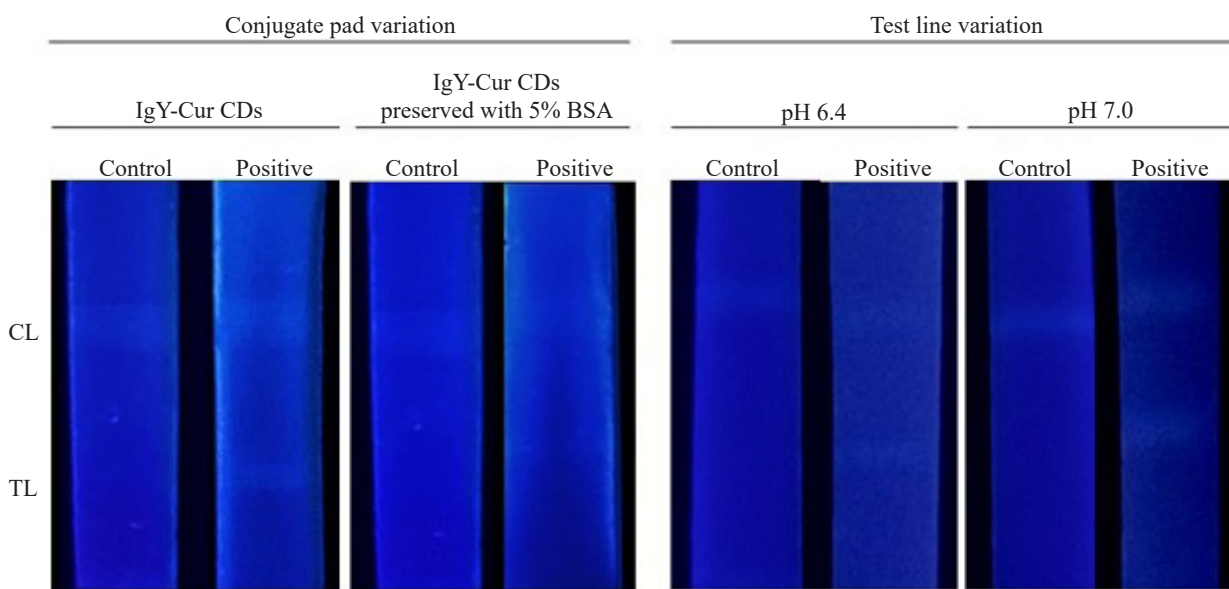


Figure 9. Feasibility test optimization using a conjugate pad and pH level of IgY antibodies immobilization on test line

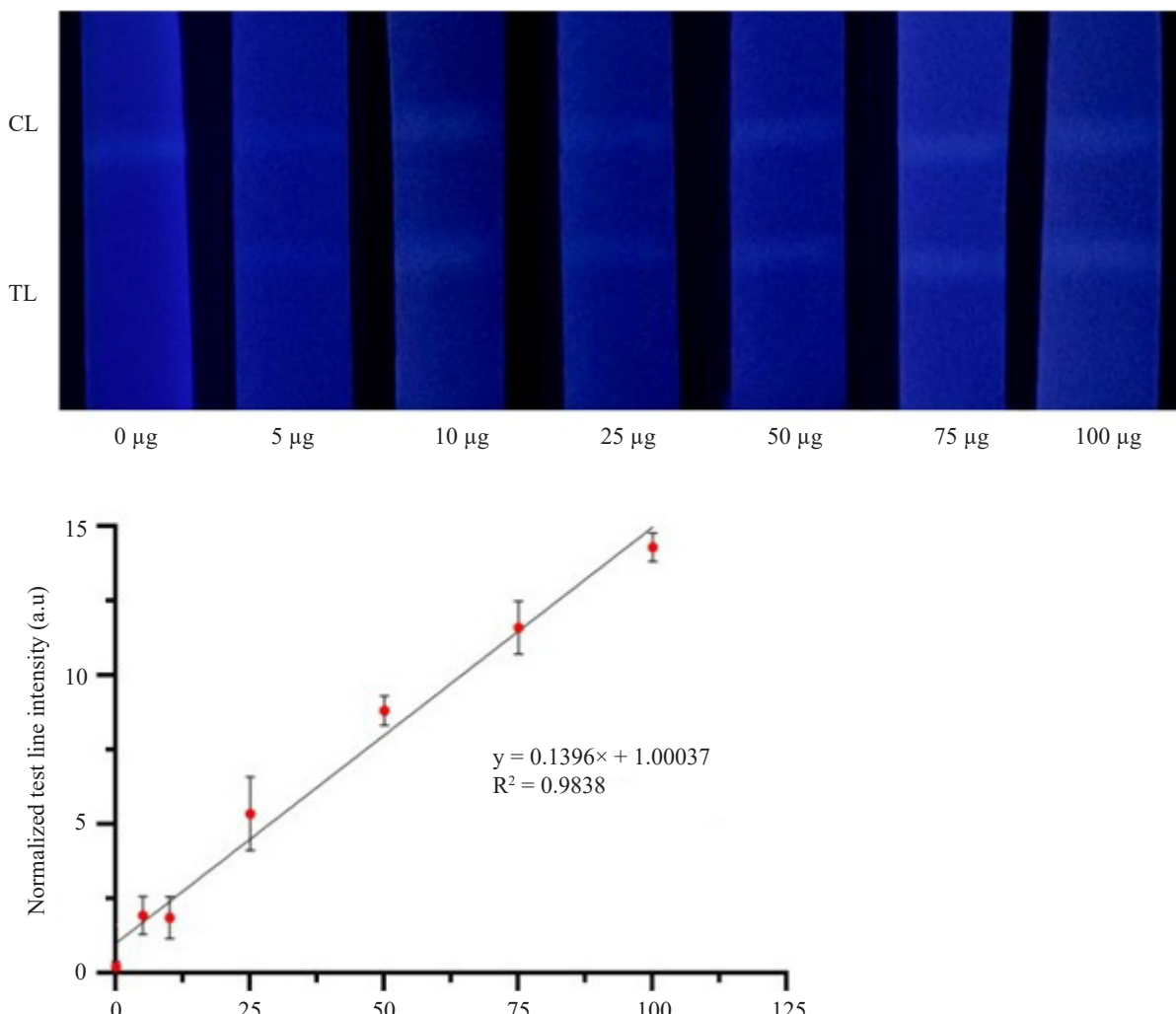


Figure 10. The sensitivity performance of the curcumin-CDs-based fluorescence LFIA for synthetic SARS-CoV-2 antigens

same concentration (10 µg). Strips stored at 25°C showed stability for only one week, failing to detect antigens in week two. In contrast, strips stored at 4°C maintained stability for three weeks, likely due to improved protein preservation at lower temperatures. In the stability test over four weeks, good results were also obtained when the samples were stored at 4°C, as indicated by consistent results (Figure 11).

3.4. Detection in Human Samples

The sensitivity test of the fluorescence LFIA was conducted by testing the strips with nasopharyngeal swab samples from confirmed COVID-19 patients. This preliminary evaluation aimed to determine the ability of the strip to accurately detect the presence of SARS-CoV-2 antigens in human samples, assessing its potential for rapid COVID-19 diagnosis. Positive patient samples produced two fluorescence lines, indicating a positive result, while

nuclease-free water, used as the negative control, showed only one line (Figure 12). These results were consistent with PCR findings using the Fosun 2019-nCoV RT-qPCR kit, where a cycle threshold of < 36 confirmed COVID-19 positivity—indicating that the CDs-based lateral flow assay of human samples is reliable.

4. Discussion

The results of the nano-bioconjugation of curcumin carbon dots (Cur CDs) with IgY, achieved through the carbodiimide carboxylamine coupling method, were characterized using various techniques, including morphological analysis, fluorescence studies, and identification of functional groups. There was an increase in the size of Cur CDs after nano-bioconjugation, and a significant trend was observed in the red shifting of emission peaks with an increase in excitation wavelength in photoluminescence spectroscopy. That

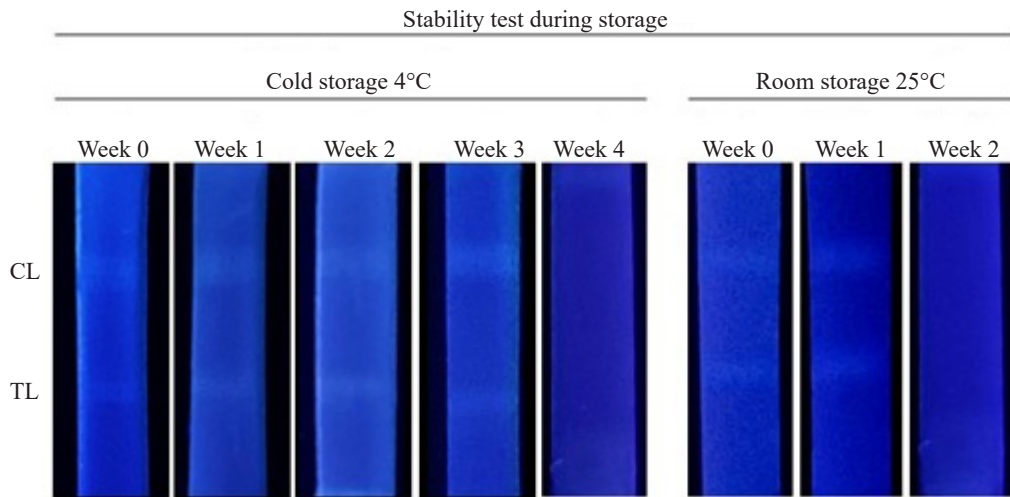


Figure 11. The stability performances under different storage temperatures (a) room temperature 25°C and (b) cold storage 4°C

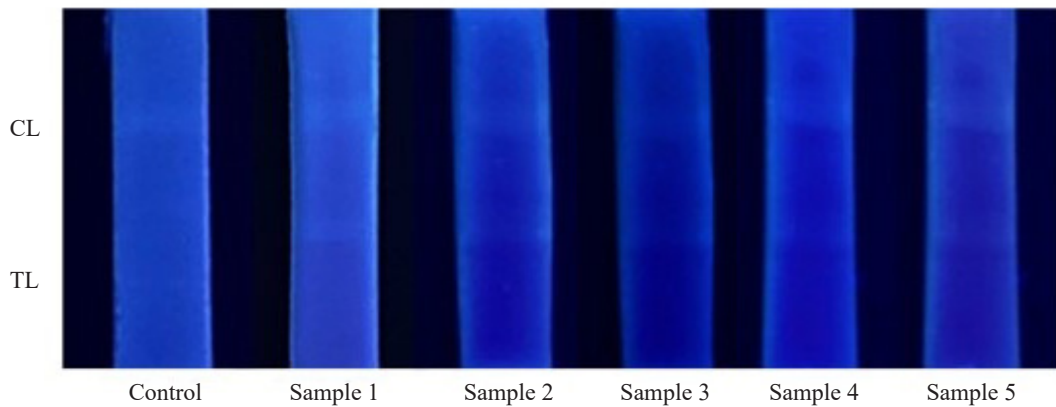


Figure 12. Real samples analysis to evaluate the sensitivity of CDs-based lateral flow test strip

result demonstrates that the structural and surface modifications of Cur CDs, resulting from conjugation with IgY antibodies, led to an increase in size and suggested changes in the electronic environment of the CDs, which affected their fluorescence shift properties (Đorđević *et al.* 2022; Kamel *et al.* 2022). EDC and NHS in this study used coupling agents that activated carboxyl groups on CDs, which were then conjugated with the amino functionalities of antibodies to form Cur CDs-IgY (Fu *et al.* 2023). These characterizations provided insights into the structural integrity, fluorescence properties, and successful conjugation of functional groups between the curcumin CDs and antibodies.

The evaluation of IgY-Cur CDs conjugates as a prior detection method for SARS-CoV-2 antigen has been revised in terms of the principle of fluorescence immunoassays. The energy transfer of donor-acceptor pairs between IgY and CDs curcumin with the addition of graphene causes the damping of fluorescence properties. The absence of antigen on the FRET immunoassay will cause Cur CDs-pAb to be absorbed onto the graphene surface via π - π bonds and hydrogen bonds between the COOH/OH groups on graphene and the amine groups on the antibodies (Huang *et al.* 2018). The intensity of fluorescence and the concentration of viral antigens increase. By increasing the concentration of viral antigen, the interaction between IgY-Cur CDs and graphene is disrupted, and the fluorescence is restored due to the specific binding affinity of IgY antibodies toward the viral antigen. This immunocomplex formation is so strong that it generates a distance between Cur CDs and graphene, which then disrupts the binding ability on their surface (Zhang *et al.* 2021). Any changes affecting the distance between the donor-acceptor molecules will impact the fluorescence phenomenon, allowing the presence of antigen to cause fluorescence recovery. Thus, the FRET immunoassay approach can be used to screen whether curcumin CDs-labeled IgY antibodies can detect various concentrations of multiepitope synthetic SARS-CoV-2 antigens as low as 10 ng.

The IgY-Cur CDs conjugate, which was successfully confirmed and optimized in the fluorescence-based LFA construct, demonstrated a detection limit of 54.28 μ g with an operational time of 35 minutes. The detection limit was calculated using the same method as previously described (Lee *et al.* 2023). While the detection limit remains relatively high compared to fluorescence-based LFIA utilizing CDs aggregation induced by the SARS-CoV-2 spike protein (Ju *et al.* 2022), this study provides foundational insight. It highlights the potential

of IgY antibodies labeled with curcumin-derived CDs as fluorescence markers in SARS-CoV-2 lateral flow immunoassays (LFIA), as evidenced by the observed increase in fluorescence intensity with higher sample concentrations.

These findings align with the well-known challenges in LFIA assembly. While much of the development process focuses on identifying the optimal construct or selecting the most suitable antigen or antibody, hidden challenges often arise from the complexity of the device itself. The intricate design of LFIA, composed of multiple interconnected elements, introduces critical considerations such as material incompatibility and defects at overlapping junctions (Koczula & Gallotta 2016). Micro-gaps between elements that should be seamlessly connected can disrupt the flow rate of the target analyte from the sample to the test line, thereby affecting the accuracy of the test. Similarly, the relatively short storage stability observed in this study may be attributed to inconsistencies in biomolecule immobilization on the cellulose membrane surface, likely caused by inadequate instrumentation.

In Conclusion, In this study, we successfully initiated the development of a fluorescence immunoassay based on Cur CDs-labeled IgY antibody for SARS-CoV-2 detection. The ability of the FRET immunoassay to exhibit the presence of viral antigen is significantly different compared to the absence of viral antigen ($p < 0.05$) with a minimum sample concentration that can detect as low as 10 ng. This evaluation, as a screening method for Cur CDs-IgY conjugates, is capable of being used as a probe. The further application of Cur CDs in constructing LFA as a fluorescence label is feasible, with an operational time of 35 minutes. This LFA performed effectively detected both synthetic multiepitope spike and NS3 SARS-CoV-2 antigens with a detection limit of 54.28 μ g/mL, as well as swab samples from confirmed COVID-19 patients. Thus, IgY-Cur CDs in this study demonstrate potential for further development as fluorescence labels in the LFA diagnostic kit. Furthermore, this research needs to be reproduced using better instruments, following standard medical device manufacturing methods. Evaluation of specificity against competing antigens is required to ensure that the LFIA accurately detects the target SARS-CoV-2 antigens without interference from other similar antigens.

Acknowledgements

We acknowledge this study was funded by the Ministry of Research, Technology, and Higher Education

of Indonesia under the "Penelitian Kompetensi Riset Dasar Nasional" program, as well as the Indonesian Endowment Fund for Education and the Indonesian Science Fund through the International Collaboration RISPRO funding program.

References

Abdillah, O.B., Floweri, O., Mayangsari, T.R., Santosa, S.P., Ogi., T., Iskandar, F., 2020. Effect of H_2SO_4/H_2O_2 pre-treatment on electrochemical properties of exfoliated graphite prepared by an electro-exfoliated method. *RSC Advances.* 18, 100881. doi:10.1039/d0ra10115j

Bhushan, B., Kumar, S.U., Gopinath, P., 2016. Multifunctional carbon dots as efficient fluorescent nanotags for tracking cells through successive generations. *Journal of Materials Chemistry B.* 4. doi:10.1039/C6TB01178K

Borghei, Y.S., Morteza, H., Mohammad, R.G., Saman, H., 2018. A novel BRCA1 gene deletion in human breast carcinoma MCF-7 cells through FRET between quantum dots and silver nanoclusters. *Journal of Pharmaceutical and Biomedical Analysis.* 152, 81-88. doi:10.1016/j.jpba.2018.01.014

Deb, A., Gaurav, R.N., Devasish, C., 2023. Biogenic carbon dot-based fluorescence-mediated immunosensor for the detection of disease biomarker. *Analytica Chimica Acta.* 1242, 340808. doi:10.1016/j.aca.2023.340808

Dorđević, L., Francesca, A., Michele, C., Maurizio, P.A., 2022. Multifunctional chemical toolbox to engineer carbon dots for biomedical and energy applications. *Nature Nanotechnology.* 17, 112-130. doi:10.1038/s41565-021-01051-7

Fibriani, A., Nugrahapraja, H., Siregar, A.L.F., Mayorga, C.G.D., Gunawan, C., Yamahoki, N., 2022. Fusion peptide as a multiepitope peptide-based COVID-19 vaccine. [Patent]. Indonesia: Institut Teknologi Bandung.

Fibriani, A., Taharuddin, A.A.P., Stephanie, R., Yamahoki, N., Laurelia, J., Wisnuwardhani, P.H., Agustiyanti, D.F., Angelina, M., Rubiyana, Y., Ningrum, R.A., Wardiana, A., Iskandar, F., Permatasari, F.A., Rachmadn, E.A.G., 2023. Carbon-dots as a potential COVID-19 antiviral drug. *Heliyon.* 9, e20089. doi:10.1016/j.heliyon.2023.e20089

Fibriani, A., Naisanu, K., Yamahoki, N., Kinanti, D.R., 2025. Development of polyclonal chicken egg yolk immunoglobulin Y (IgY) antibodies targeting SARS-CoV-2 multiepitope antigen. *Journal of Virological Methods.* 331, 115062. doi:10.1016/j.jviromet.2024.115062

Fu, C., Qin, X., Zhang, J., Zhang, T., Song, Y., Yang, J., Wu, G., Luo, D., Jiang, N., Bikker, F.J., 2023. *In vitro* and *in vivo* toxicological evaluation of carbon quantum dots originating from *Spinacia oleracea*. *Heliyon.* 9, e13422. doi:10.1016/j.heliyon.2023.e13422

Huang, A., Zhang, L., Li, W., Ma, Z., Shuo, S., Yao, T., 2018. Controlled fluorescence quenching by antibody-conjugated graphene oxide to measure TAU protein. *Royal Society Open Science.* 5, 171808. doi:10.1098/rsos.171808

Huang, C., Dong, H., Su, Y., Wu, Y., Narron, R., Yong, Q., 2019. Synthesis of carbon quantum dot nanoparticles derived from byproducts in bio-refinery process for cell imaging and *in vivo* bioimaging. *Nanomaterials.* 9, 387. doi:10.3390/nano9030387

Ju, J., Zhang, X., Li, L., Regmi, S., Yang, G., Tang, S., 2022. Development of fluorescent lateral flow immunoassay for SARS-CoV-2-specific IgM and IgG based on aggregation-induced emission carbon dots. *Frontiers in Bioengineering and Biotechnology.* 10, 1042926. doi:10.3389/fbioe.2022.1042926

Kamel, M., Maher, S., El-Baz, H., Salah, F., Sayyouh, O., Demerdash, Z., 2022. Non-invasive detection of SARS-CoV-2 antigen in saliva versus nasopharyngeal swabs using nanobodies conjugated gold nanoparticles. *Tropical Medicine and Infectious Disease.* 7, 102. doi:10.3390/tropicalmed7060102

Koczula, K.M., Gallotta, A., 2016. Lateral flow assays. *Essays in Biochemistry.* 60, 111-120. doi:10.1042/EBC20150012

Kuznetsova, H., Géloën, A., Dziubenko, N., Zaderko, A., Alekseev, S., Lysenko, V., Skryshevsky, V., 2023. In vitro and *in vivo* toxicity of carbon dots with different chemical compositions. *Discover Nano.* 18. doi:10.1186/s11671-023-03891-9

Lee, A.S., Kim, S.M., Kim, K.R., Park, C., Lee, D.G., Heo, H.R., Cha, H.J., Kim, C.S., 2023. A colorimetric lateral flow immunoassay based on oriented antibody immobilization for sensitive detection of SARS-CoV-2. *Sensors and Actuators B: Chemical.* 379, 133245. doi:10.1016/j.snb.2022.133245

Pan, Y., Wei, X., 2022. A novel FRET immunosensor for rapid and sensitive detection of dicofol based on bimetallic nanoclusters. *Analytica Chimica Acta.* 1224, 340235. doi:10.1016/j.aca.2022.340235

Raveendran, V., Kizhakayil, R.N., 2021. Fluorescent carbon dots as biosensor, green reductant, and biomarker. *ACS Omega.* 6, 23475-23484. doi:10.1021/acsomega.1c03481

Tang, Z., Liu, X., Su, B., Chen, Q., Cao, H., Yun, Y., Xu, Y., Hammock, B.D., 2020. Ultrasensitive and rapid detection of ochratoxin A in agro-products by a nanobody-mediated FRET-based immunosensor. *Journal of Hazardous Materials.* 387, 121678. doi:10.1016/j.jhazmat.2019.121678

Tang, J., Wu, L., Lin, J., Zhang, E., Luo, Y., 2021. Development of quantum dot-based fluorescence lateral flow immunoassay strip for rapid and quantitative detection of serum interleukin-6. *Journal of Clinical Laboratory Analysis.* 35, e23752. doi:10.1002/jcla.23752

Verma, A.K., Noumani, A., Yadav, A.K., Solanki, P.R., 2023. FRET based biosensor: Principle applications recent advances and challenges. *Diagnostics.* 13, 1375. doi:10.3390/diagnostics13081375

Wang, J., Meng, H.M., Chen, J., Liu, J., Zhang, L., Qu, L., Li, Z., Lin, Y., 2019. Quantum dot-based lateral flow test strips for highly sensitive detection of the tetanus antibody. *ACS Omega.* 4, 6789-6795. doi:10.1021/acsomega.9b00657

WHO coronavirus disease (COVID-19) dashboard. Available at <https://covid19.who.int/table> [Date accessed: 30 March 2023]

Xu, L.D., Zhu, J., Ding, S.N., 2021. Immunoassay of SARS-CoV-2 nucleocapsid proteins using novel red emission-enhanced carbon dot-based silica spheres. *Analyst*. 146, 5055-5060. doi:10.1039/D1AN01010G

Zhang, R., Jin, Z., Tian, Z., Liu, Y., Lu, Z., Cui, Y., 2021. A straightforward and sensitive "on-off" fluorescence immunoassay based on silicon-assisted surface enhanced fluorescence. *RSC Advances*. 11. doi:10.1039/D0RA08759A